# The effect of Ku on telomere replication time is mediated by telomere length but is independent of histone tail acetylation

Hui-Yong Lian[a,*], E. Douglas Robertson[a,*,†], Shin-ichiro Hiraga[a], Gina M. Alvino[b], David Collingwood[c], Heather J. McCune[b,‡], Akila Sridhar[a], Bonita J. Brewer[b], M. K. Raghuraman[b], and Anne D. Donaldson[a]

[a]Institute of Medical Sciences, University of Aberdeen, Foresterhill, Aberdeen AB25 2ZD, Scotland, UK; Departments of [b]Genome Sciences and [c]Mathematics, University of Washington, Seattle, WA 98195

**ABSTRACT** **DNA replication in *Saccharomyces cerevisiae* proceeds according to a temporal program. We have investigated the role of the telomere-binding Ku complex in specifying late replication of telomere-proximal sequences. Genome-wide analysis shows that regions extending up to 80 kb from telomeres replicate abnormally early in a *yku70* mutant. We find that Ku does not appear to regulate replication time by binding replication origins directly, nor is its effect on telomere replication timing mediated by histone tail acetylation. We show that Ku instead regulates replication timing through its effect on telomere length, because deletion of the telomerase regulator Pif1 largely reverses the short telomere defect of a *yku70* mutant and simultaneously rescues its replication timing defect. Consistent with this conclusion, deleting the genome integrity component Elg1 partially rescued both length and replication timing of *yku70* telomeres. Telomere length–mediated control of replication timing requires the $TG_{1–3}$ repeat-counting component Rif1, because a *rif1* mutant replicates telomeric regions early, despite having extended $TG_{1–3}$ tracts. Overall, our results suggest that the effect of Ku on telomere replication timing results from its impact on $TG_{1–3}$ repeat length and support a model in which Rif1 measures telomere repeat length to ensure that telomere replication timing is correctly programmed.**

**Monitoring Editor**
Orna Cohen-Fix
National Institutes of Health

Received: Jun 29, 2010
Revised: Feb 7, 2011
Accepted: Mar 7, 2011

## INTRODUCTION

DNA replication in eukaryotes initiates from multiple chromosomal loci called replication origins. In *Saccharomyces cerevisiae*, potential replication origin sites are termed autonomously replicating sequence (ARS) elements and are largely specified by DNA sequence (Nieduszynski *et al.*, 2006). Replication initiation is tightly controlled to ensure that each origin initiates, or "fires," no more than once during each S phase. Initiation of replication does not occur simultaneously at all origins but rather according to a temporal program. Some origins initiate replication at the onset of S phase, and others only later (Reynolds *et al.*, 1989; Ferguson *et al.*, 1991), as revealed by microarray-based genome-wide studies (Raghuraman *et al.*, 2001; Yabuki *et al.*, 2002; McCune *et al.*, 2008). Such genome-wide studies facilitated the identification of replication origins as the earliest-replicating sequences in their chromosome localities.

Chromosomal context is important for determining the processional order of origin firing (Ferguson and Fangman, 1992; Friedman *et al.*, 1996; Raghuraman *et al.*, 1997). For example, regions within 35 kb of a telomere typically replicate later in S phase than the genomic average (Raghuraman *et al.*, 2001), and proximity to a telomere is one of the chromosome contexts that tends to cause late origin initiation. Telomere-specified late replication is dependent on the presence of the chromosome end—that is, telomeric sequences placed in the context of a circular plasmid do not delay replication (Ferguson and Fangman, 1992). Two telomeric

This article was published online ahead of print in MBoC in Press (http://www.molbiolcell.org/cgi/doi/10.1091/mbc.E10-06-0549) on March 25, 2011.

*These authors contributed equally to this work.

Present addresses: †Department of Surgery & Molecular Oncology, Ninewells Hospital, University of Dundee, Dundee DD1 9SY, Scotland, UK; ‡700 Steiner St., #503, San Francisco, CA 94117.

Address correspondence to: Anne D. Donaldson (a.d.donaldson@abdn.ac.uk).

Abbreviations used: ARS, autonomously replicating sequence; ChIP, chromatin immunoprecipitation; dUTP, 2′-deoxyuridine, 5′-triphosphate; HH, heavy-heavy; HL, heavy-light; qPCR, quantitative PCR.

protein complexes have been implicated in specifying late replication close to telomere V-right—the Sir silencing complex (consisting of Sir2, Sir3, and Sir4 proteins) and the Ku complex (a heterodimer consisting of Yku70 and Yku80 subunits that binds to DNA ends, including double-stranded breaks and telomeres) (Stevenson and Gottschling, 1999; Cosgrove *et al.*, 2002). Of these, the Ku complex has the greater effect, affecting the replication time of both subtelomeric sequences (such as Y′ elements) and telomere-proximal replication origins (such as *ARS522*, previously called *ARS501*, which is located 27 kb from chromosome V-right) (Cosgrove *et al.*, 2002). The *yku70* mutation causes abnormally early telomere replication, possibly through a combined effect on origin initiation time and efficiency (Cosgrove *et al.*, 2002).

We do not understand in molecular terms how cells control the replication timing program, but there is evidence suggesting that chromatin organization or modification plays an important role. In particular, it was shown that increased histone H4 K12 N-terminal tail acetylation in an *rpd3* mutant, which lacks a major cellular histone deacetylase, correlates with an advancement in origin replication time (Vogelauer *et al.*, 2002; Aparicio *et al.*, 2004; Knott *et al.*, 2009). Moreover, tethering the histone acetyltransferase Gcn5 close to a normally late-initiating replication origin resulted in increased histone H3 lysine 18 acetylation and earlier initiation of the origin in S phase (Vogelauer *et al.*, 2002). These experiments showed that changes in histone tail acetylation state can alter replication timing, suggesting a mechanism for determining the timing program. Perhaps surprisingly, however, there is no clear relationship in vivo between the level of histone tail acetylation at origins and their replication times (Nieduszynski *et al.*, 2006).

Evidence is emerging for a link between the mechanisms that control telomere length maintenance and replication timing. A recent investigation showed that shortening a telomere early in the cell cycle, using a system in which telomere repeat sequences are recombinationally excised, causes it to replicate earlier in the subsequent S phase (Bianchi and Shore, 2007). This study established a connection between the length of a telomere and its time of replication, but provided no suggestion as to the mechanism by which telomere length can affect initiation of a replication origin tens of kilobases distant.

Here we examine the replication program of a *yku70* mutant genome-wide. In the absence of Yku70 function, at most chromosome ends a region extending up to 80 kb from the telomere replicates earlier than in wild-type cells. In contrast, internal chromosome loci generally maintain their normal replication time. To test whether the effect of Ku on the replication timing of telomeric regions is mediated by histone N-terminal tail acetylation, we used chromatin immunoprecipitation (ChIP) to examine histone acetylation at replication origin sites that show an altered replication time. We observed no effect of the y*ku70* mutation on acetylation of the histone 4 tail or H3 lysine 18 at such telomere-proximal origins, suggesting that Ku affects origin replication time through a mechanism that is independent of these histone modifications. Next we tested whether the effect of Ku on replication timing is related to telomere length. Combining *yku70* with the telomere-elongating mutations *pif1* or *elg1* led to rescue of both telomere length and replication timing defects, suggesting that the effect of the *yku70* mutation on replication timing is mediated by telomere shortening. Analysis of the replication program of a *rif1* mutant suggests that telomere length measurement by the $TG_{1–3}$ repeat binding protein Rif1 is critical for control of replication timing by telomere terminal repeat length. Our results support the idea of a close functional relation between telomere length maintenance and replication timing (Bianchi and Shore, 2007).

## RESULTS

### Yeast telomeres replicate earlier in the *yku70* mutant

In the absence of Ku complex, certain telomeric regions replicate abnormally early in S phase (Cosgrove *et al.*, 2002). We wished to examine the range of the effect of Ku on chromosome ends, whether all telomeres were affected, and whether any other regions of the genome alter their replication time in the absence of Ku complex. To address these questions, we used a microarray-based method previously used to examine *S. cerevisiae* genomic replication dynamics (Raghuraman *et al.*, 2001). Our modification to the approach used isotopic labeling of newly replicated DNA to measure the proportion of each genomic sequence that has been replicated when a culture is in the middle of S phase. *YKU70*$^+$ ("wild type") or *yku70* mutant cells were grown in medium containing heavy isotopes of carbon and nitrogen, arrested before S phase, and then released in isotopically light medium (Figure 1A). For each culture, a large sample was taken at a predetermined mid-S phase time point (25 min after release). Replicated heavy-light (HL) DNA was separated from unreplicated heavy-heavy (HH) DNA by cesium chloride gradient fractionation. Replicated and unreplicated DNA fractions were fluorescently labeled, pooled, and hybridized to genomic microarrays. The representation of each genomic sequence in the HL and HH DNA fractions depends on its time of replication: The earliest-replicating sequences will already have moved to the HL DNA fraction at mid-S phase, whereas late-replicating sequences remain in the HH fraction (Raghuraman *et al.*, 2001). We found that the percentage replication of each sequence at mid-S phase shows an inverse linear relationship to its replication time (Supplemental Figure S1), allowing the array-based percentage replication measurements to be plotted as proxies for replication times of each sequence in S phase (see *Materials and Methods*). Specimen plots obtained for chromosomes III, V, and VI are shown in Figure 1B. A comparison with previous data sets is shown in Supplemental Figure S2, and wild-type and *yku70* replication timing plots for the entire genome are presented in Supplemental Figure S3. To assemble these plots, the raw (% replicated) data were subjected to Fourier convolution and sliding window smoothing (Alvino *et al.*, 2007) before further processing as described in *Materials and Methods*, including transformation to replication time ($T_{rep}$) based on the graphs in Supplemental Figure S1A.

The replication timing plots reveal that, in general, the replication dynamics of the *yku70* mutant closely mirror those of wild-type cells throughout internal chromosomal regions. Most telomeric regions, however, replicate noticeably earlier in *yku70* than in wild type (with the chromosome ends earlier by an average of 6.0 ± 1.3 min). For example, loci within 35 kb of the right end of chromosome III replicate between 6 and 10 min earlier in the *yku70* mutant than in wild type (Figure 1B). Loci close to the right end of chromosome V replicate 6–7 min earlier in *yku70* than in wild type, consistent with previous observations (Cosgrove *et al.*, 2002). These differences are apparent even without correction for the ~3-min delay shown by *yku70* mutants in entering S phase after release from α-factor (see Cosgrove *et al.*, 2002, and axes in Figure 1B plots). The magnitude of the replication time advancement varies among telomeres (see Supplemental Table S2) and extends variable distances into the interior of the chromosome arms. Plotting the difference in replication time between wild type and *yku70* against distance from the closest telomere for all genomic loci (Figure 2A) confirms that the largest differences in replication timing are observed at the chromosome ends. The effect on replication timing decreases gradually with increasing distance from telomeres, so that replication times of loci more than 80 kb from a telomere are almost unaffected by the *yku70* mutation.

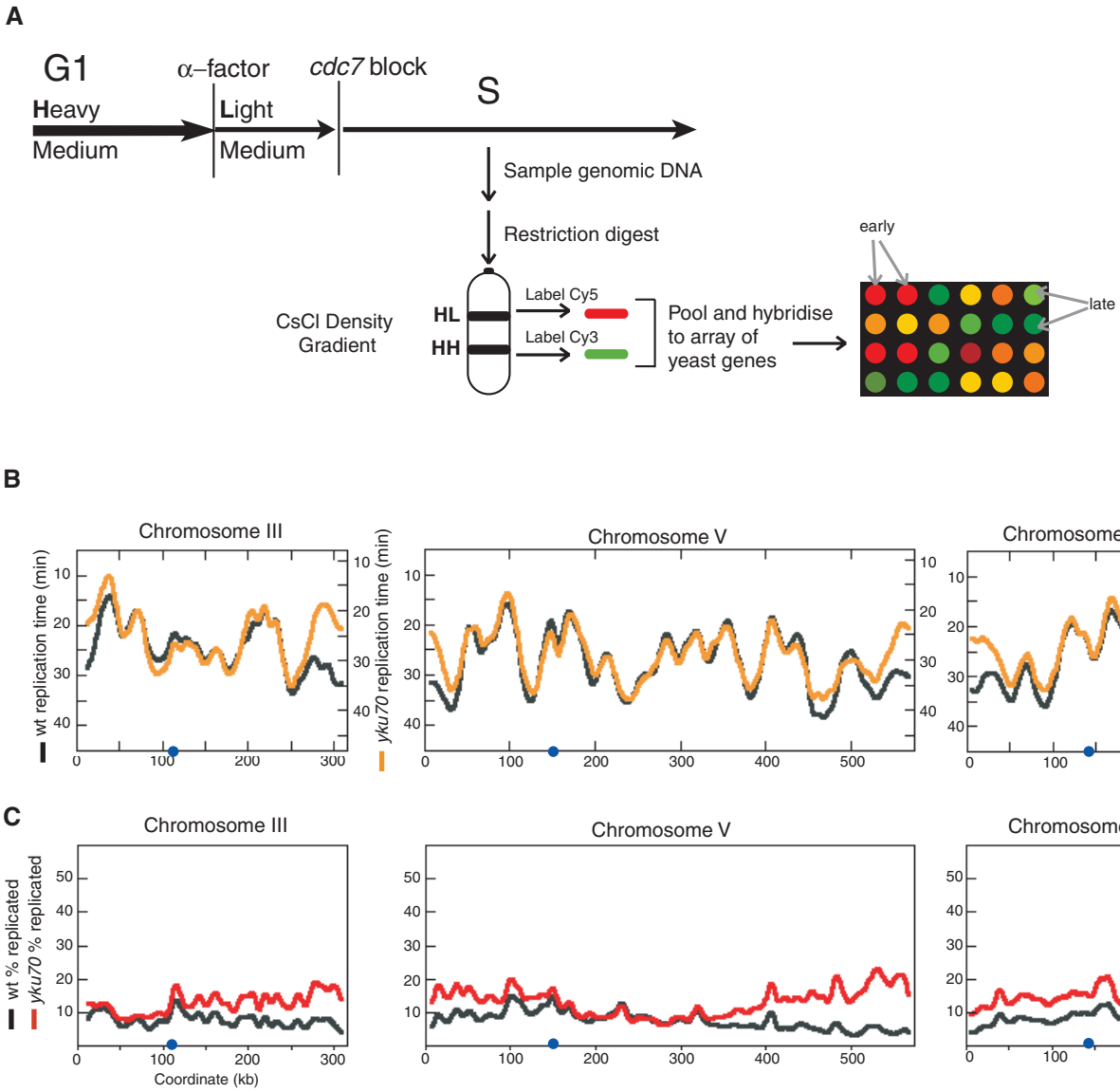


FIGURE 1: Yeast telomeres replicate earlier in the *yku70* mutant. (A) Outline of experimental procedure, as described in the text. (B) Plots showing replication time of chromosomal loci on chromosomes III, V, and VI, in *YKU70*$^+$ ("wt"; black line, left-hand axes) and *yku70* mutant (orange line, right-hand axes). The *yku70* mutant shows a reproducible 3-min delay when compared with wild type in entering S phase after release from a *cdc7* block; *y* axes are offset by 3 min for easier comparison of the replication timing profiles. Centromere positions are marked by blue dots. (C) Plots showing the percentage of cells in the population that have replicated chromosomal loci on chromosomes III, V, and VI at the zero time point (*cdc7* block) in wild type (black line) and *yku70* mutant (red line). Blue dots indicate centromere positions.

The variability seen in the effect of *yku70* on different chromosome ends may reflect the particular configuration of nearby replication origins and their time and efficiency of activation. In many cases, the change in replication timing could be explained by an effect of Ku on the X and/or Y′ ARS elements within the subtelomeric repeat sequences, which, because of their repetitive nature, are not represented in the microarray profiles. Analysis of a truncated chromosome V-right construct lacking the X and Y′ ARS elements demonstrated that the *yku70* mutation also advances the initiation time of the telomere-proximal origin *ARS522* (Cosgrove *et al.*, 2002). Supplemental Figure S3 timing profiles suggest that, in several other telomeric regions, origins at some distance from the chromosome end show advanced time of activation (in particular, at I-left, III-left and -right, IV-right, and XII-right)—indicating that in these cases at least, the effect of Ku extends tens of kilobases and probably affects multiple origins. Two early-replicating origin sites located fairly close to chromosome ends (37.5 kb from telomere III-left and 28 kb from telomere IX-right) also displayed an advancement in replication time in *yku70*, although the effects on these origins were reduced in magnitude compared with late origins. Figure 2B plots the replication timing difference at all origin sites identified within 100 kb of a telomere. Most origins within 40 kb of a telomere showed an advancement in replication time in *yku70*, with the magnitude of the effect generally reflecting the proximity of the origin to the chromosome end. The one exception was an origin located 28 kb from the chromosome XIII-right telomere, the replication time of which was unaltered in *yku70*. At distances greater than 50 kb from telomeres, the effects of the *yku70* mutation on origin replication time appeared

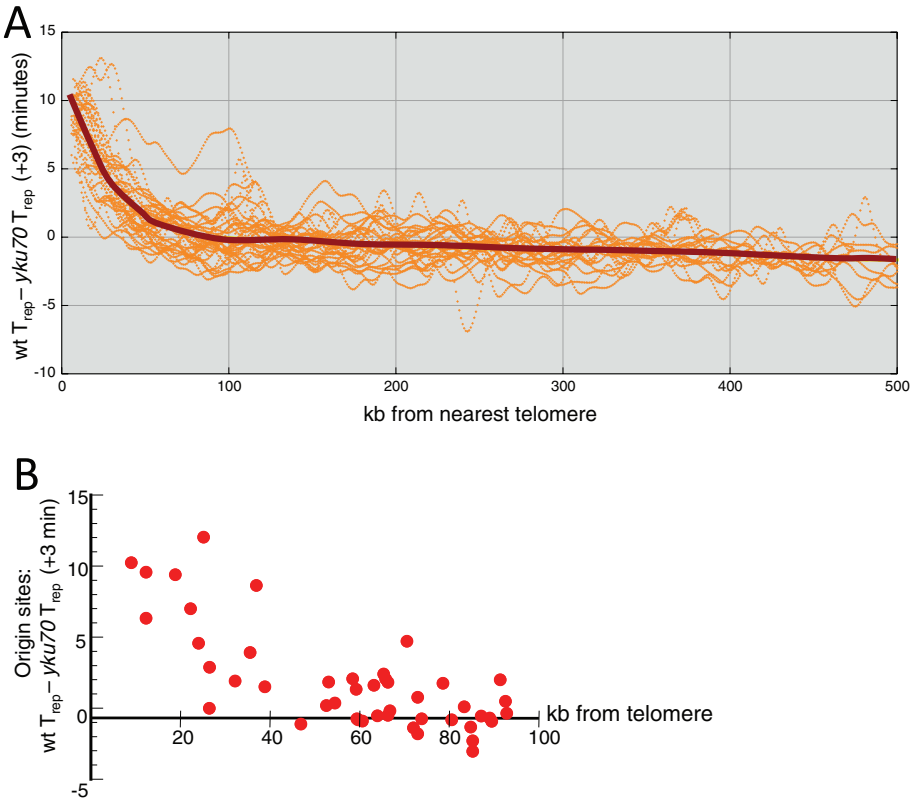


FIGURE 2: Effect of telomere proximity on replication timing in *yku70*. (A) Dot plot shows the difference in replication time ($T_{rep}$) between wild type and *yku70*, plotted against distance from the closest telomere. Points are at 1-kb intervals for all genomic loci within 500 kb of a telomere; dark red line shows curve fit. (B) Dot plot showing replication time difference between wild type and *yku70* at all origin sites identified within 100 kb of a telomere. For both plots, values are corrected for the 3-min delay of the *yku70* strain in entering S phase.

minimal (Figure 2B). The fact that the effect of the *yku70* mutation on replication timing propagates somewhat further than its effect on origins is as expected, because earlier origin initiation will cause an advancement in replication time of all sequences within that replicon, including those on the centromere-proximal side of the origin. To summarize, the results of our genome-wide replication timing analysis confirmed that the Ku complex causes telomeric regions to replicate late and showed that Ku has no general effect on the replication temporal program of internal chromosomal domains.

### Effect of *cdc7* synchronization on replication timing

In the microarray replication timing experiments, the cultures were synchronized using sequential α-factor and *cdc7* temperature blocks. Low levels of "escape" replication are seen from certain very early-initiating replication origins (e.g., *ARS306*) in cells depleted of Cdc7 activity in both control and *yku70* mutant strains (Reynolds *et al.*, 1989; Donaldson *et al.*, 1998a). Interestingly, microarray-based analysis of zero-time-point (i.e., *cdc7* blocked) samples showed that telomeric regions in the *yku70* strain are particularly prone to escape replication (Figure 1C and Supplemental Figure S4). The data plotted in Figure 1B, Supplemental Figure S3, and Figure 2 have been corrected (as described in Reynolds *et al.*, 1989), to subtract the effects of escape replication from the proportion of replicated DNA in mid-S phase. The effect of *yku70* on telomere replication time is apparent even after correcting for escape replication; therefore the *yku70* mutation can be regarded as having two separate effects on replication dynamics of telomere-proximal regions: It causes an increase in their escape replication at a *cdc7* block (as shown in Figure 1C and Supplemental Figure S4) and separately advances their replication time within S phase (as shown in Figure 1B and Supplemental Figure S3).

The effect of the *yku70* mutation appeared more extensive on chromosome I than on other chromosomes (Supplemental Figure S3). More detailed analysis of the replication dynamics of a nontelomeric origin site at ~70 kb on chromosome I (corresponding to *ARS106*; Nieduszynski *et al.*, 2007) confirmed that this locus replicates earlier in the *yku70* mutant strain and shows pronounced escape replication (Figure 3, A and C). *ARS106* replication was, however, not advanced in *yku70* when only α-factor (and not the *cdc7* block) was used for synchronization (Figure 3, B and C), in contrast to telomeric sequences. It is unclear why chromosome I behaves differently from other chromosomes, but this observation suggests that the more extensive effects of *yku70* on chromosome I replication dynamics may be related to use of the *cdc7* block.

### Ku complex is not present at telomere-proximal replication origins

Ku has been detected as binding only within 7.5 kb of telomeres (Martin *et al.*, 1999) but can affect the replication time of origins up to 40 kb distant from a telomere (Figure 2 and Cosgrove *et al.*, 2002). We investigated possible mechanisms by which Ku might exert this long-range effect on the replication timing of telomere-proximal replication origins. It has been suggested that the Ku heterodimer may bind replication origins in both yeast and mammalian cells (Shakibai *et al.*, 1996; Novac *et al.*, 2001), so we tested whether Ku affects telomere-proximal replication origins by binding them directly. ChIP was used to enrich for Yku80-bound DNA regions, and the sequences recovered were measured using quantitative PCR (qPCR). We first examined Yku80 binding at two control sequences close to telomere VI-right (Figure 4A). High levels of Yku80 binding to a sequence 300 bp from telomere VI-right were observed, as expected because Ku is known to bind telomeres. Slight, residual binding of Ku80 was observed at a sequence 5 kb from telomere VI-right (Figure 4A), but analysis of sites more distant from the chromosome end did not suggest any spreading of Ku farther from the telomere (unpublished data). A *yku70* Yku80-Myc strain served as a "no binding" control, because Yku80 binds DNA only as an obligate heterodimer with Yku70 (Griffith *et al.*, 1992; Ono *et al.*, 1994). Yku80 binding to the telomere region was completely lost in this control strain, as expected.

We examined Ku binding at three telomere-proximal replication origins within regions showing advanced replication time in the absence of Ku function: *ARS609* (14 kb from the chromosome VI-right telomere), *ARS316* (43 kb from the chromosome III-right telomere), and *ARS522* (27 kb from the chromosome V-right telomere). Our ChIP analysis revealed no significant enrichment of Yku80 at any of these telomere-proximal replication origins in log phase cell cultures (Figure 4A). The residual signal obtained at *ARS609*, *ARS316*, and

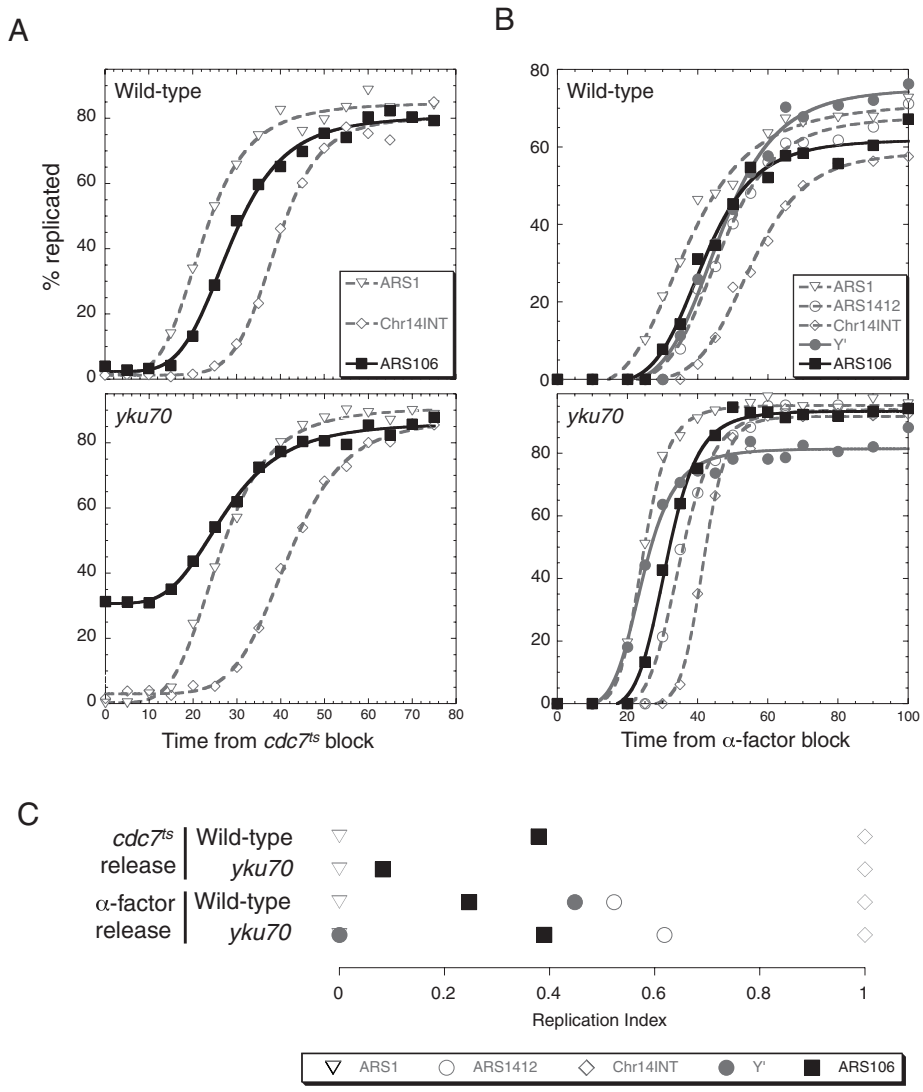


FIGURE 3: Replication dynamics of *ARS106* locus on release from *cdc7*$^{ts}$ block or from α-factor block. (A) Plots show kinetics of replication of three different sequences in wild type (top panel) and *yku70* (bottom panel) strains after release from *cdc7*$^{ts}$ block, measured using slot blot analysis of the proportions of replicated and unreplicated DNA throughout S phase. Replication kinetics are plotted for early origin *ARS1* (open triangles), an internal late-replicating sequence on chromosome XIV (open diamonds), and *ARS106* (black squares). Strains are KK14–3a and AW101. (B) Replication of five different sequences in wild type (top panel) and *yku70* (bottom panel) strains after release from α-factor block, measured using slot blot analysis of the proportions of replicated and unreplicated DNA throughout S phase. Replication kinetics are plotted for early origin *ARS1* (inverted open triangles), subtelomeric Y′ sequences (gray circles), internal late origin *ARS1412* (open circles), an internal late-replicating sequence on chromosome XIV (open diamonds), and *ARS106* (black squares). Strains are BB14–3a and AW99. (C) Relative replication times of sequences in the experiments shown in parts A and B, plotted as Replication Index values (i.e., with replication times of early marker sequence *ARS1* and late marker sequence chromosome XIV-internal set to 0 and 1, respectively).

*ARS522* was similar to that found for nonorigin and internally located sequences (unpublished data). To test for a transient interaction of Ku with affected origins occurring only during replication, ChIP experiments were also carried out using synchronized cultures (Figure 4B). Even in mid-S phase cells, we observed no significant interaction of Ku80 with *ARS522* (Figure 4C) or *ARS609* (Supplemental Figure S5).

Overall, we find no evidence for binding of the Ku complex to replication origin sites. Although we cannot rule out the possibility of an interaction undetectable by ChIP, these results indicate that Ku is unlikely to influence the replication timing of telomeric regions by interacting directly with telomere-proximal origins.

### No change in histone 4 or histone 3 N-terminal tail acetylation in *yku70*

Alterations to histone tail acetylation levels in nucleosomes surrounding replication origins can affect their initiation time (Yabuki *et al.*, 2002; Aparicio *et al.*, 2004). We investigated whether altered histone tail acetylation close to telomere-proximal replication origins in the *yku70* mutant might account for their altered replication timing. First, we tested whether the N-terminal tail of histone H4 shows increased acetylation in *yku70* at telomere-proximal origins in ChIP experiments using an acetylated H4-specific antibody (raised against an H4 peptide acetylated at lysines 5, 8, 12, and 16). The antibody was first tested in Western blots to confirm its specificity (Figure 5A). As expected, mutating the four target lysine residues to glycine abolished antibody recognition of histone H4. Esa1 is an H4-specific acetylase and, in a temperature-sensitive *esa1–414* mutant, the level of histone H4 acetylation is reduced at the restrictive temperature (Clarke *et al.*, 1999). The antibody did not recognize histone H4 in the *esa1–414* mutant at the restrictive temperature of 37°C, confirming its specificity for the acetylated form of histone H4 (Figure 5A). Conversely, the Western blot signal was increased by deletion of the histone deacetylase Rpd3, further confirming specificity for acetylated forms of histone H4.

We used this acetylation-specific antibody to test for a change in histone H4 acetylation corresponding to the observed change in replication time. In *yku70*, H4 acetylation levels were unaffected (i.e., within experimental error) at origin *ARS609* and at loci 500 bp on either side (Figure 5B). This result suggested that altered H4 tail acetylation in the *ARS609* region does not account for the change in replication dynamics of the telomere VI-right region in *yku70*. Ku function is required for the establishment of telomeric silencing through Sir2-mediated histone deacetylation in regions close to (generally within ~4 kb of) telomeres (Robyr *et al.*, 2002). We did observe approximately threefold increased recovery in the *yku70* mutant of a sequence at the chromosome VI-right telomere (Figure 5B, 300 bp), confirming that we were able to detect changes in histone H4 acetylation state. The increased acetylation that we observed at the end of chromosome VI-right in *yku70* is likely due to the reduced recruitment of the repressive Sir complex that contains the histone H4 lysine 16 deacetylase Sir2.

Examination of other telomere-proximal origins, *ARS316* and *ARS522*, which showed precocious replication in the *yku70* mutant,

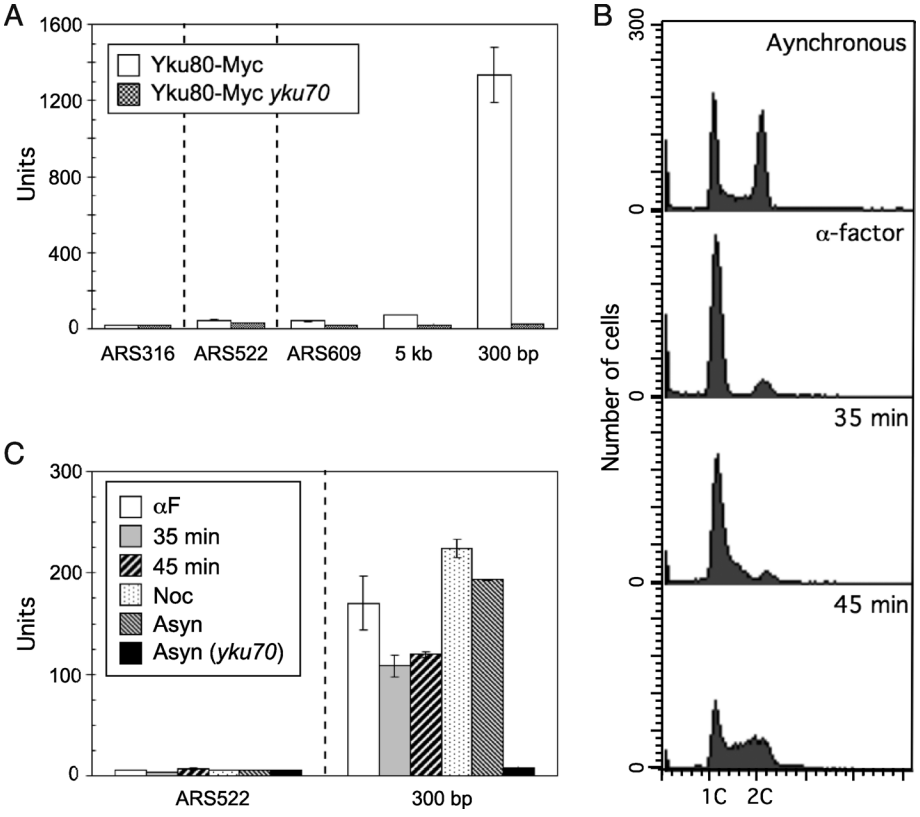


FIGURE 4: Ku does not bind replication origins directly. (A) qPCR analysis of DNA sequences immunoprecipitated from asynchronously growing log phase cultures of Yku80-Myc (SHY167) and Yku80-Myc *yku70* (DR2) strains using an anti-Myc monoclonal antibody (mAb) (ab56; Abcam). Primers were designed to amplify sequences that cover the ARS Consensus Sequences of *ARS316*, *ARS522*, and *ARS609* and sequences located 5 kb and 300 bp from the right end of chromosome VI. Results are expressed relative to a standard genomic DNA dilution series as described in *Materials and Methods*. (B) Flow cytometry analysis of Yku80-Myc (SHY167) strain on release from α-factor block shows that the culture is in mid-S phase 45 min following release. (C) Analysis of Ku80 binding to *ARS522* and locus 300 bp from telomere VI-right in synchronized cells. ChIP-qPCR was carried out as described in part (A), using Yku80-Myc (SHY167) cultures blocked with α-factor, 35 min after release, 45 min after release, blocked with nocodazole, and growing asynchronously. ChIP-qPCR analysis of asynchronously growing Yku80-Myc *yku70* (DR2) strain provides a negative control for comparison.

likewise revealed no significant change in histone H4 acetylation (Figure 5C). We conclude that regulation of histone H4 tail acetylation close to telomere-proximal replication origins is unlikely to be the mechanism by which Ku affects their initiation time.

Artificially increasing histone H3 acetylation levels by tethering the histone acetyltransferase Gcn5 has also been shown to cause an advancement in the replication time of a late origin (Vogelauer *et al.*, 2002). Tethered Gcn5 was shown to affect acetylation levels of H3 Lys-18. We therefore examined whether acetylation of H3 Lys-18 is altered at telomere-proximal replication origins in *yku70*. The specificity of a commercial anti-H3K18Ac antibody was checked in Western blots against protein extracts from an *rpd3* histone deacetylase mutant and a strain in which H3 Lys-18 had been mutated to arginine (Figure 5D). The results confirmed that the antibody reactivity toward H3 is ablated in an H3K18R mutant. Mutation of neighboring lysines in the H3 tail also compromised antibody recognition, which could indicate either some cross-reactivity with other H3 acetylation sites or that acetylation of these lysine residues is coordinated (with a mutation at one lysine residue affecting acetylation of those nearby). Having confirmed that its primary specificity is against acetylated H3 Lys-18, we used this antibody in ChIP experiments to examine histone H3 Lys-18 acetylation levels at *ARS316*, *ARS522*, and *ARS609* (Figure 5E). We observed no significant difference in acetylation of H3 Lys-18 at or close to any of these origins. On the basis of this result, we conclude that deacetylation of the histone H3 Lys-18 residue is not the mechanism by which Ku regulates the replication time of telomere-proximal origins.

In ChIP experiments to examine histone acetylation state (such as those shown in Figure 5), it is possible that high-density nucleosomes that have a low level of acetylation could produce a signal equal to that from lower density, more highly acetylated nucleosomes. To test whether changes in acetylation state at telomere-proximal origins might be "masked" by altered nucleosome occupancy, we examined histone H3 association with telomere-proximal replication origin loci using an antibody against unmodified histone 3 (Supplemental Figure S6A). We found no change in the level of histone H3 occupancy in the *yku70* mutant close to *ARS316* (Supplemental Figure S6B) or other telomere-proximal replication origins (unpublished data). The failure to observe increased histone acetylation at telomere-proximal origins in *yku70* therefore does not result from reduced nucleosome occupancy.

### Rescuing telomere length in the *yku70* mutant restores late telomere replication

The *yku70* mutant has short telomeres, caused by defects in telomerase recruitment and telomere capping (Peterson *et al.*, 2001; Maringele and Lydall, 2002; Stellwagen *et al.*, 2003; Fisher *et al.*, 2004). Telomere shortening has been shown to lead to earlier telomere replication (Bianchi and Shore, 2007). To test whether the effect of *yku70* on telomere replication time is caused by its shortened telomeres, we examined the effect of deleting the *PIF1* gene. Pif1 is a 5′ to 3′-directed helicase that negatively regulates telomere length. Pif1 limits telomerase processivity by unwinding of the RNA:DNA hybrid involved in $TG_{1\text{-}3}$ tract extension (Zhou *et al.*, 2000; Boule *et al.*, 2005; Bochman *et al.*, 2010). Loss of this helicase activity causes *pif1* single mutants to have elongated telomeres due to their failure to control $TG_{1\text{–}3}$ tract extension, but importantly, the telomere length sensing machinery is intact. To test whether shortened $TG_{1\text{–}3}$ tracts cause the abnormally early replication of telomeric regions in *yku70*, we deleted *PIF1*—because the double *yku70 pif1* mutant lacks Ku function, but is expected to have normal length telomeres and an intact telomere-length-sensing machinery.

We constructed a *pif1 yku70* mutant and measured telomere length using Southern blotting. Deletion of *PIF1* largely rescued the short telomere defect of the *yku70* mutant (Figure 6A); telomeres in the *yku70 pif1* strain have an average length only slightly shorter than wild type. To test whether rescuing the telomere length defect of *yku70* also leads to recovery of the normal late telomere replication time, we used the dense isotope transfer

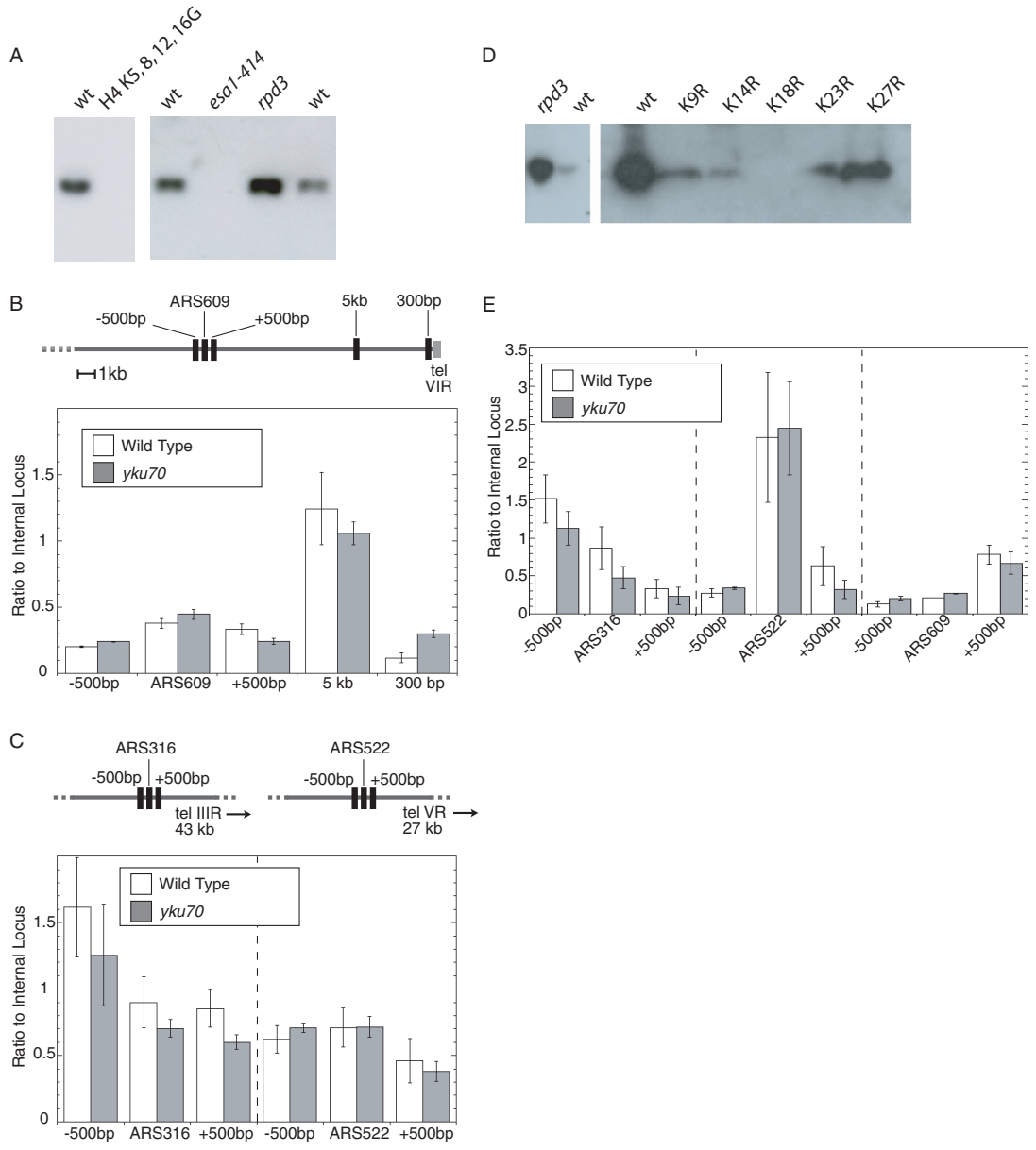


FIGURE 5: Histone tail acetylation is unchanged at telomere-proximal replication origins in the *yku70* mutant. (A) Western blots analyzing specificity of anti–tetra-acetylated histone H4 primary antibody (06–598; Upstate). In control "wild-type" (wt) extracts, the presence of a single band at ~10 kDa represents acetylated histone H4. The antibody fails to recognize histone H4 in a strain in which the four target lysines residues (K5, 8, 12, and 16) are mutated to glycine (left panel). The right panel shows the reactivity of the antibody to extracts from *esa1*$^{ts}$ and *rpd3* strains, in comparison to their respective wild-type parents. From left to right, strains are: WY130, WY129, LPY02991, LPY03291, DR3, and BY4741. Equivalent loading was confirmed by Coomassie staining (unpublished data). (B) Chromosome cartoon shows an ~20 kb region at telomere VI-right, with the location of the subtelomeric X element shown as a gray box. Locations of sequences analyzed are marked by vertical black bars. Graph shows qPCR analysis of chromatin sequences immunoprecipitated from wild type (RM14–3a) and *yku70* mutant (AW101) cells using anti–tetra-acetylated histone H4 primary antibody. Primer pairs for *ARS609*, 5 kb and 300 bp loci are those used in Figure 3, with additional pairs used to measure recovery of sequences 500 bp either side of *ARS609*. Results are expressed relative to the amplification obtained for a standard internal locus. Error bars indicate the range of values between two ChIP experiments. (C) As B, except measuring the recovery of sequences at or flanking the telomere-proximal replication origins *ARS316* and *ARS522*. (D) Western blots to examine specificity of anti–acetyl histone H3K18 primary antibody (ab1191; Abcam). In extracts from wild-type cells, a band at ~15 kDa detects acetylated histone H3. The left panel shows Western blot signal obtained from *rpd3* mutant extract (DR3), compared with the corresponding wild type (BY4741). The right-hand panel shows antibody reactivity against strains carrying the single lysine mutants K9R, K14R, K18R, K23R, or K27R (strains NSY119, NSY120, NSY130, NSY131, NSY132, respectively), compared with the corresponding wild-type strain (NSY115). Equivalent loading was confirmed by Coomassie staining (unpublished data). (E) qPCR analysis of sequences immunoprecipitated using the anti–acetyl histone H3K18 antibody from wild-type (RM14–3a) and *yku70* mutant (AW101) cells. Primer pairs are as used in parts B and C, and results are expressed in the same way. Error bars indicate the range of values between two ChIP experiments.

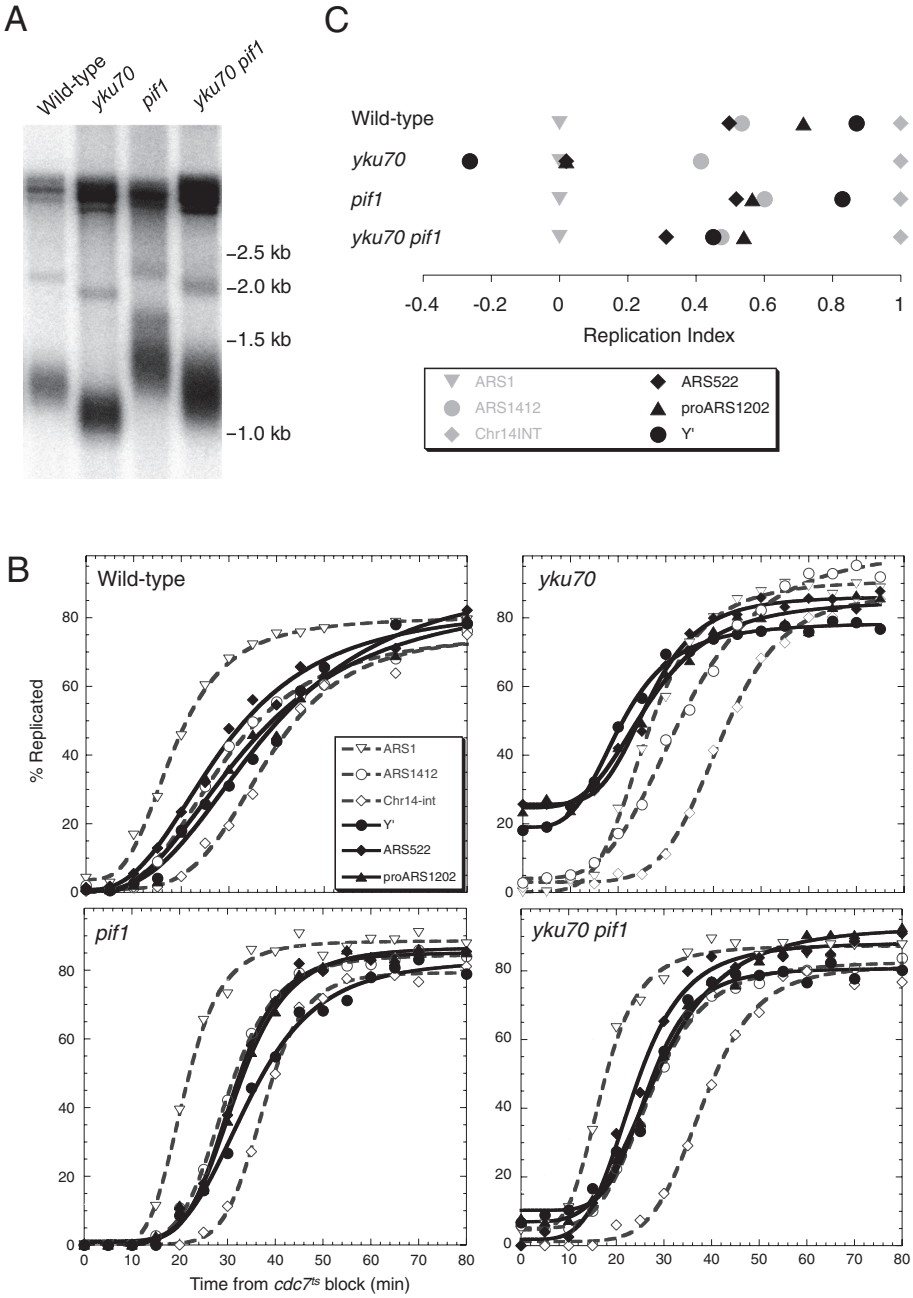


FIGURE 6: Telomere length and replication timing are restored in a *pif1 yku70* mutant. (A) *pif1 yku70* cells have terminal *Xho*I fragments of close to normal length. DNA from wild-type control, *yku70*, *pif1*, and *pif1 yku70* strains was digested with *Xho*I and analyzed by Southern blotting, using a $TG_{1-3}$ probe to detect chromosome terminal fragments. The smeared bands above the 1 kb marker correspond to telomeres containing a Y′ element. (B) Replication timing experiments showing replication kinetics of various genomic sequences after release from a *cdc7*$^{ts}$ block. Strains are RM14–3a (wild type), AW101 (*yku70*), HYLS77 (*pif1*), and HYLS68 (*yku70 pif1*). (C) Replication times of sequences from part B, plotted as Replication Index values (i.e., with replication times of early and late marker sequences set to 0 and 1, respectively).

method to examine the *yku70 pif1* replication program (Figure 6B). We measured the replication time of telomere-proximal origins *ARS522* and *proARS1202* (which lies 31 kb from telomere XII-left), as well as the average replication time of the Y′ subtelomeric repeat sequences. In a *YKU70*$^{+}$ *PIF1*$^{+}$ ("wild-type") strain, *ARS522*, *proARS1202*, and Y′ sequences all replicate at a similar time to the internal late origin *ARS1412*, but in a *yku70* mutant these telomere-proximal sequences replicate much earlier (compare with early origin *ARS1*; Figure 6B). In the *yku70 pif1* mutant, we found that all three telomere-proximal sequences reverted to a late replication time similar to that of *ARS1412*, and close to their normal time of replication. Telomeric sequences in a *pif1* single mutant replicated at close to their normal time in late S phase.

The replication time of a sequence can be assigned as the time at which replication has achieved half of its final level. Figure 6C shows the relative replication times (Replication Indices; Friedman *et al.*, 1996) of various sequences in wild type, *yku70*, *pif1*, and *yku70 pif1* strains. The replication times of telomeric markers *proARS1202*, *ARS522*, and Y′ are largely (60–80%) recovered in the *yku70 pif1* strain when compared with *yku70*, comparable with 76% recovery of telomere length (the average length of the terminal Xho1 fragment being 1280 bp in wild type, 1144 bp in *yku70*, and 1247 bp in *yku70 pif1*).

To examine further whether telomere replication timing in *yku70* is linked to telomere length, we tested the effects of combining *yku70* with other telomere-lengthening mutations (Askree *et al.*, 2004; Gatbonton *et al.*, 2006). Most of the mutations tested (such as *mlp2*, *rad5*, and *rad27*) failed to cause any elongation of the shortened telomeres of a *yku70* mutant. Likewise, expression of Cdc13-Est1 or Cdc13-Est2 proteins lengthened telomeres in wild type (Evans and Lundblad, 1999), but not in a *yku70* background (unpublished data). We did however identify one mutation, *elg1*, which caused mild (~20%) rescue of *yku70* short telomeres (Figure 7A). *ELG1* encodes the largest subunit of a Replication Factor C-like complex (Parnas *et al.*, 2010). Analyzing the replication program of the *yku70 elg1* strain revealed that the replication times of telomeric marker sequences also showed partial rescue (25% recovery of Y′, 19% of *proARS1202*, and 39% of *ARS522* replication timing; Figure 7B), consistent with the suggestion that the replication time of chromosome ends in *yku70* is linked to telomere length. Interestingly, replication of Y′ sequences showed increased asynchrony in the *yku70 elg1* mutant (Supplemental Figure S7; note shallow slope of Y′ curve), possibly reflecting the greater spread of telomere lengths observed in this mutant (Figure 7A). In conclusion, the phenotypes of both the *yku70 pif1* and *yku70 elg1* mutants suggest that telomere shortening in the *yku70* strain can account for its replication timing defect.

### Rif1 is required for late telomere replication

Analysis of the *yku70 pif1* mutant suggested that the effect of the *yku70* mutation on telomere replication timing is due to shortened

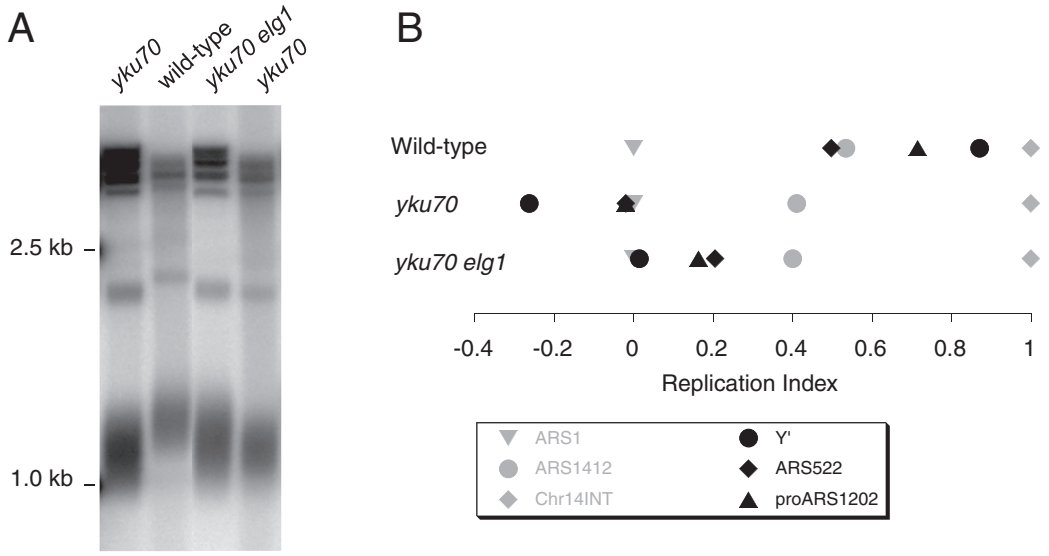


FIGURE 7: Telomere length and replication timing in an *elg1 yku70* mutant. (A) *elg1 yku70* cells have slightly longer terminal *Xho*I fragments than do *yku70* cells. DNA from wild type, *yku70*, and *elg1 yku70* strains was digested with *Xho*I and analyzed as in Figure 6A. One lane was removed from the image between wild type and *yku70 elg1* samples. (B) Replication times of sequences in wild type, *yku70*, and *yku70 elg1* strains, plotted as Replication Index values. Replication curves are shown. Strains are RM14–3a (wild type), AW101 (*yku70*), and HYLS63 (*yku70 elg1*).

telomeres. To investigate further the idea that telomere length and $TG_{1\text{-}3}$ repeat-sensing machinery are important to regulate telomere replication timing, we tested a mutant in which telomere length sensing is lost. Wild-type cells use a $TG_{1–3}$ terminal repeat–counting mechanism that controls telomerase-mediated elongation, such that short telomeres are preferentially lengthened. This counting mechanism involves $TG_{1–3}$ tract binding by Rap1, followed by recruitment of its interacting factors Rif1 and Rif2. Rif1 and Rif2 "measure" telomere length and down-regulate telomerase activity at chromosome ends with adequate $TG_{1\text{-}3}$ repeat length (reviewed by Bianchi and Shore, 2008). In a *rif1* mutant, this telomere length–sensing machinery is defective, and a *rif1* mutant has long telomeres due to failure to control telomerase and consequent uncontrolled $TG_{1–3}$ tract elongation (Figure 8A) (Hardy *et al.*, 1992; Wotton and Shore, 1997).

To assess whether telomere length measurement for replication timing control involves the same length-sensing machinery, we tested whether telomere replication time responds correctly to telomere length when $TG_{1–3}$ tract sensing is defective—that is, in a *rif1* mutant. If Rif1 is required to detect long telomeres and in response specify late initiation of nearby origins, then we would predict that *rif1* telomeric regions would replicate early, because cells will be unable to detect their elongated $TG_{1–3}$ tracts. If, in contrast, Rif1 is not involved in controlling telomere replication timing, then the expectation is that the elongated telomeres of a *rif1* mutant would cause its chromosome ends to replicate at the normal late time (or possibly even later than normal).

We tested the replication-timing program of a *rif1* mutant (Figure 8B). We found that telomere-proximal origins *ARS522* and *proARS1202* both replicate substantially earlier than normal, at approximately the same time as the early origin *ARS1* (Figure 8, B and C). The average replication time of Y′ sequences is also much earlier in *rif1* than in the wild-type control. In a *rif1* mutant, telomeric and telomere-proximal sequences therefore replicate abnormally early, despite their excessively long $TG_{1–3}$ tracts. We conclude that Rif1 is part of the pathway that senses $TG_{1–3}$ tract length and relays that information to telomere-proximal origins to specify their replication time. A *rif1 yku70* double mutant also replicated its telomeres early despite their almost normal length, consistent with loss of the length-sensing machinery.

## DISCUSSION

In this study we have examined the effect of deleting Ku on the *S. cerevisiae* temporal program of DNA replication. We discovered that Ku can influence replication timing of chromosome ends over a long range, affecting the replication time of sequences up to 80 kb from telomeres. Our genome-wide study showed that the *yku70* mutation affects the replication timing of all telomeres to some extent. The effect on some telomeres extends over tens of kilobases, but on others (e.g., XIII-right, XV-right) the effect is restricted to the chromosome end. The extent of the effect on replication timing may reflect the number, configuration, and normal initiation time of replication origins close to each telomere.

One caveat in interpreting microarray-based replication timing data arises from the presence of nonunique sequences within the terminal 20–30 kb of many chromosomes arms (23 of the 32 telomeres falling into groups sharing some degree of homology; Louis, 1995). Such similarity compromises the uniqueness of some microarray probes, so that the replication timing data for some chromosome ends must be interpreted with caution. We focused on chromosome VI-right in several experiments because it contains unique sequence to within ~500 bp of the chromosome end, permitting reliable probe and primer design.

We tested whether Ku modulates telomere replication dynamics by affecting nucleosome modifications that have previously been implicated in control of replication timing—namely, acetylation of the histone N-terminal tails at residues H4K5, 8, 12, and 16 or H3K18. We did not detect changes in acetylation of these residues at telomere-proximal replication origins that account for the effects of *yku70* on replication initiation, suggesting that the advancement in replication time of telomere regions in *yku70* is independent of histone tail acetylation. It remains possible that a different chromatin modification might be involved in mediating the effect of Ku on initiation time of telomere-proximal origins (Pryde *et al.*, 2009).

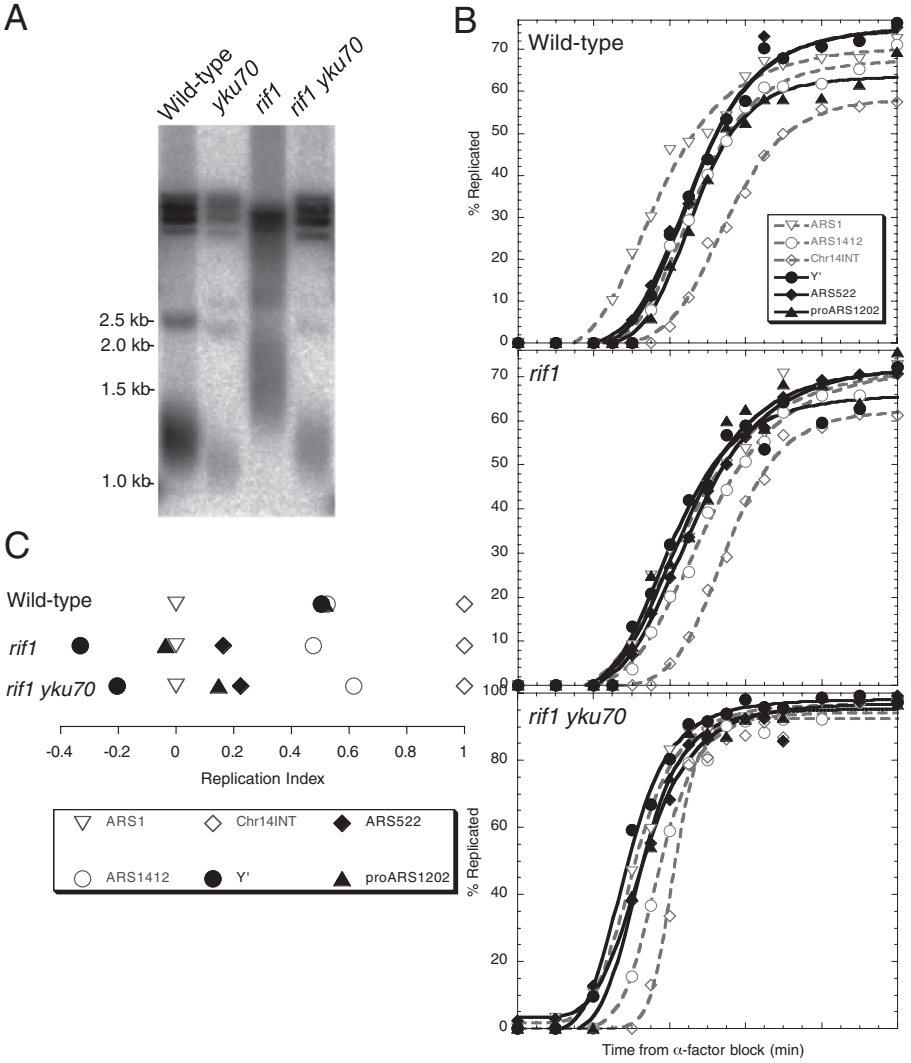


FIGURE 8: Telomere-proximal sequences replicate abnormally early in *rif1*. (A) Telomere length is extended in *rif1* cells. DNA from *rif1* and wild type (*RIF1*$^{+}$) control strains was digested with *Xho*I and analyzed by Southern blotting, using a $TG_{1–3}$ probe to detect chromosome terminal fragments. The smeared bands between 1 and 2 kb in length correspond to telomeres containing a Y′ element. (B) Replication kinetics of various genomic sequences after release from α-factor of wild type, *rif1*, and *rif1 yku70* strains. (C) Replication times of sequences from part B, plotted as Replication Index values. Variation between Figures 6 and 8 in wild-type replication time and Replication Index values probably reflects differing synchronization protocols (i.e., release from α-factor block, which was essential here for technical reasons but typically gives lower resolution of replication times than *cdc7*$^{ts}$ release). Strains are BB14–3a (wild-type), HYLS44 (*rif1*), and HYLS46 (*rif1 yku70*).

Loss of Ku function has several effects on yeast telomere organization that could potentially be related to the replication timing defect. Specifically, deletion of *YKU70* causes loss of normal telomere positioning at the nuclear periphery, failure of subtelomeric transcriptional silencing, and abnormally short telomeres (Boulton and Jackson, 1998; Laroche *et al.*, 1998; Stellwagen *et al.*, 2003). Deregulated telomere replication timing in *yku70* does not appear to be due to defective telomere subnuclear positioning (because other mutants that derail telomere positioning do not affect replication timing; Hiraga *et al.*, 2006) or to the telomeric silencing defect (because deleting Sir components has a milder effect than *yku70* on telomere replication timing; Stevenson and Gottschling, 1999; Cosgrove *et al.*, 2002). We created a *pif1 yku70* mutant to examine whether the replication timing defect of cells lacking Ku can be rescued by restored telomere length. We found that a *pif1 yku70* strain has telomeres of almost normal length and that they replicate at close to their normal late time in S phase. Because *pif1 yku70* mutant cells lack Ku function but have restored telomere length and replication timing, this observation suggests that the effect of the *yku70* mutation on telomere replication timing is most likely a consequence of telomere shortening. Consistent with this suggestion, the *yku70 elg1* mutant showed slight rescue of telomere length and similarly mild restoration of replication timing.

Our observations are consistent with those from the Shore laboratory demonstrating that an engineered short telomere is reprogrammed to replicate early. Specifically, recombinational excision during G1 of a subtelomeric $TG_{1–3}$ tract causes early replication of that telomere in the subsequent S phase (Bianchi and Shore, 2007). The effects of such artificial telomere truncation on replication appear similar to those of the *yku70* mutation: In particular, either the *yku70* mutation or engineered shortening results in advancement of the replication time of both subtelomeric replication origin sequences (i.e., those within X and Y′ elements) and telomere-proximal origins, such as *ARS522* (Cosgrove *et al.*, 2002; Bianchi and Shore, 2007).

How is information on telomere length relayed to telomere-proximal replication origins? To begin to address this question, we tested whether the Rif1 protein, which has a central role in measuring $TG_{1–3}$ tract length to regulate telomerase activity, is also involved in measuring $TG_{1–3}$ tract length to control replication timing. Both *pif1* and *rif1* mutants have elongated telomeres but for completely different reasons: An important difference between these mutants is that the *pif1* mutant has intact telomere length–sensing machinery, whereas in a *rif1* mutant this machinery is defective. We found that a *rif1* strain replicates its telomere-proximal sequences early despite its greatly extended terminal $TG_{1–3}$ tract length, suggesting that *rif1* cells lack the ability to transmit telomere length information to nearby replication origins (as well as failing to repress telomerase activity at long telomeres). Figure 9 illustrates our model for the role of Rif1 in telomere length–controlled replication timing in wild-type and mutant strains. The most likely explanation for the early replication of *rif1* telomeres is that, without Rif1 protein, cells lack the machinery required to detect their long telomeres and program the initiation time of nearby replication origins accordingly (Figure 9D). In other words, in the absence of Rif1 the cells constitutively interpret their terminal $TG_{1–3}$ tracts as being critically short, and so engage the mechanism that causes short telomeres to replicate early.

Our findings do not address the mechanism by which telomere-associated Rif1 protein transmits information to replication origins

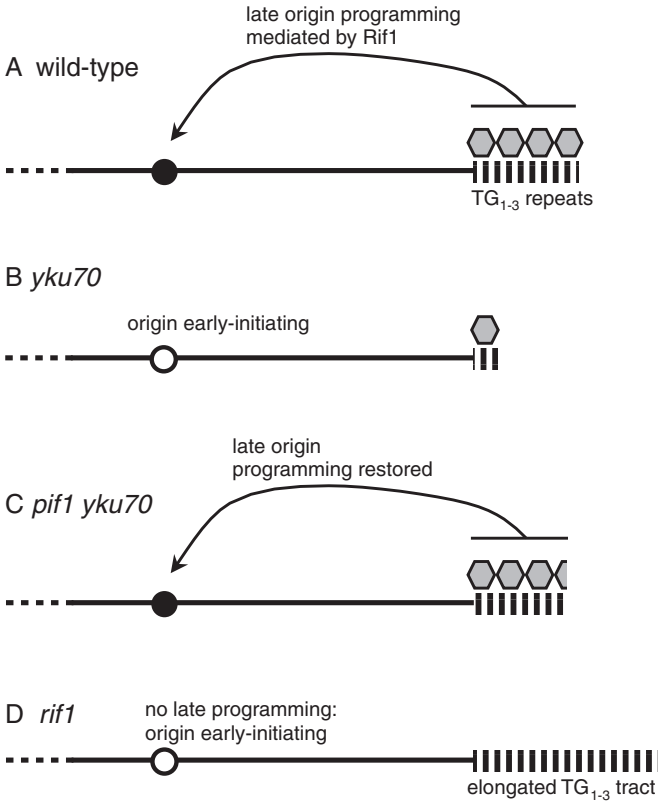


FIGURE 9: Model of replication timing control by Rif1-mediated telomere length measurement. (A) In wild-type cells, terminal $TG_{1–3}$ tract length is "counted" by activated Rif1 molecules (gray hexagons). If $TG_{1–3}$ repeat length is sufficient, Rif1 relays a signal to nearby origins (such as telomere-proximal Y′ or *ARS522* origins) specifying their late replication time (black circle). (B) In *yku70*, $TG_{1–3}$ tract length is short due to compromised telomerase recruitment and telomere uncapping. $TG_{1–3}$ repeat length is insufficient for activated Rif1 to cause late origin programming, so a nearby origin initiates early (white circle). (C) In *pif1 yku70* $TG_{1–3}$ repeat length is restored, activating sufficient Rif1 to allow late origin programming. (D) A *rif1* mutant lacks the Rif1-mediated "count-and-delay" mechanism, with the result that nearby origins initiate replication early despite their extended $TG_{1–3}$ repeat length.

that may (like *ARS522*) lie tens of kilobases distant from the chromosome end. Our results suggest that the effect of *yku70* (and telomere length) on replication timing is not mediated by altered acetylation state of the histone H3 or H4 tails. Although changes in histone tail acetylation clearly can affect replication origin initiation (Vogelauer *et al.*, 2002), they do not appear to mediate the long-range effect of telomeres on replication timing. In their study of the effects of deacetylase Rpd3 and HAT Gcn5 on replication dynamics, Vogelauer *et al.* concentrated on internal late replication domains and did not examine telomere-proximal origins. One possibility therefore is that histone tail acetylation state mediates origin initiation time within internal late replication domains (distant from telomeres), but a different mechanism (not acting through histone tail acetylation) mediates the effect of telomeres on replication timing. We propose that the programming of replication time close to chromosome ends occurs through a Rif1-dependent mechanism in which $TG_{1–3}$ tract length is measured, and the information is fed into an unidentified pathway that controls replication initiation time. We are investigating the possibility that, as well as measuring $TG_{1–3}$ tract length, an activated form of Rif1 itself transmits the telomere-length signal to replication origins, regulating replication initiation through an effect on the Cdc7 kinase replication initiation factor. Such a role for *S. cerevisiae* Rif1 in replication control could be related to the reported function of the human Rif1 homologue, which is involved in regulating DNA replication of heterochromatic domains (Buonomo *et al.*, 2009). Understanding the pathways by which yeast telomeres affect the replication program of nearby sequences will elucidate the links between telomere biology and replication and may help uncover general mechanisms that regulate DNA replication.

## MATERIALS AND METHODS

### Yeast strains

Genotypes and sources of the strains used are listed in Supplemental Table S1. Mutated alleles were created by targeted PCR-based gene knockout, with correct transformants verified by PCR according to standard procedures.

### Replication timing analysis

The replication time of specific sequences was measured using the dense isotope transfer procedure (McCarroll and Fangman, 1988; Donaldson *et al.*, 1998b), probing for specific genomic *Eco*RI fragments as described previously (Cosgrove *et al.*, 2002). *ARS106* replication time was measured by probing for a 4956 bp *Eco*RI restriction fragment (coordinates 66359–71315) on chromosome I.

### Analysis of percent replication and replication time

Genome-wide replication timing analysis was performed in a *MATa cdc7$^{ts}$* strain background using an adaptation of the procedure described by Raghuraman *et al.* (2001). *yku70* (AW101) and control *YKU70$^{+}$* (KK14–3a) strains grown in isotopically heavy medium were presynchronized using α-factor, transferred into isotopically light medium containing α-factor, then released from α-factor at 37°C and allowed to proceed to a *cdc7$^{ts}$* block. Cultures were released into S phase by transferring to a 23°C shaker. Two series of small-volume samples were taken throughout S phase for flow cytometry analysis and to allow measurement of replication kinetics of specific sequences using standard slot blot hybridization as previously described (McCarroll and Fangman, 1988; Cosgrove *et al.*, 2002). From each culture two large samples were taken for array analysis, the first at the *cdc7* block (0 min) and the second at a mid-S phase point (25 min after release). From these samples genomic DNA was prepared and digested with *Eco*RI, after which HL (replicated) DNA was separated from HH (unreplicated) by cesium chloride gradient centrifugation. The replicated and unreplicated DNA fractions were recovered and separately labeled with Cy5-dUTP (2′-deoxyuridine, 5′-triphosphate) or Cy3-dUTP (Amersham Biosciences, Piscataway, NJ) before pooling and hybridizing to glass slide microarrays, on which each open reading frame was represented by a PCR fragment (GEO platform accession number GPL1914; Fred Hutchinson Cancer Research Center, Seattle, WA). After quality control and removal of unreliable points from the data files, the raw %HL values were assembled into chromosome plots and subjected to norma lization and smoothing using a 10-kb sliding window as described (Raghuraman *et al.*, 2001; Alvino *et al.*, 2007).

Approximately equal amounts of HH and HL DNA were used in each array hybridization. For culture samples in which the actual percentage of replicated DNA lay outside the range of 40–60% of total DNA (i.e., in the zero-time-point samples, in which the actual percentage of replicated DNA was typically 10–20%), data processing included a global normalization step to adjust the total proportion of signal generated by HL DNA to the experimentally determined value, obtained by hybridizing fractions from the appropriate cesium

chloride gradient with a probe containing whole genomic DNA. All plots were additionally corrected for "noncycling" cells (i.e., for the proportion of HH DNA contributed by cells that failed to release from the *cdc7* block, determined by analyzing final replication levels in each experiment) (Alvino *et al.*, 2007). Next the smoothed "%HL" curves were converted into "% replicated" curves (i.e., corrected for the doubling of each sequence when it replicates) using the equation:

$$\%\text{replication} = [50 \times \%\text{HL}]/[100 - (\%\text{HL}/2)]$$

This analysis produced a series of plots showing the percentage of cycling cells that had replicated each sequence in that sample. For the zero-time-point samples, these plots of "% replicated" are shown in Figure 1C and Supplemental Figure S4.

The elevated levels of replication at the zero time point in extended telomere-proximal domains in the *yku70* mutant (Supplemental Figure S4) caused a relative overrepresentation of the latest-replicating sequences in the HL DNA fraction in the mid-S phase samples (unpublished data). This overrepresentation in turn affected the gradients of the *yku70* plots at very-late-replicating loci within telomere-proximal regions, causing a misleading apparent "acceleration" of replication forks toward replication termination zones. To correct for this effect, and to allow separate assessment of the effects of Ku complex on "escape" (zero time point) replication and S phase replication time, the % replication values at mid-S phase were corrected for zero-time-point replication as described (Reynolds *et al.*, 1989).

We assessed the relationship between percent replication as measured from the mid-S phase (25 min) samples and replication time in S phase, using replication timing values obtained for individual sequences by conventional slot blot analysis (Supplemental Figure S1). A linear relationship was observed for both wild-type and *yku70* experiments, allowing the equations describing the lines in Supplemental Figure S1A to be used to transform the 25-min percent replication values into replication times, facilitating comparison of the curves with each other and with previous data sets. The resulting plots of replication time in S phase are presented in Supplemental Figure S3 and Figure 1B.

Plots show the mean of two hybridizations. The terminal 5 kb was deleted from each end of all chromosome plots to remove end-related artifacts in the data processing and analysis. The results obtained in this study were highly consistent with those from previous analyses that used slightly different strategies to measure replication dynamics (Raghuraman *et al.*, 2001; Alvino *et al.*, 2007; see comparative plot in Supplemental Figure S2).

Origin sites were assigned using criteria similar to those described (McCune *et al.*, 2008). SD values in the microarray-derived data were estimated based on the zero-time-point percent replicated curves in wild type, converted to their equivalent replication times. In this case, to be called an origin site, a peak was required to rise 2.5 SD values above the surrounding valleys in both wild-type and *yku70* mutant plots. Peaks were required to lie within 7.5 kb to be taken to correspond to the same origin (based on the estimated resolution for this type of study; Raghuraman *et al.*, 2001; Nieduszynski *et al.*, 2007). These fairly strict criteria strengthen the likelihood that differences observed reflect initiation timing differences (as opposed to efficiency differences) but exclude some likely origin sites, particularly those close to chromosome ends where the data set may terminate close to the origin. Several apparent origins the initiation times of which appear to be affected by the *yku70* mutation (e.g., XII-left ~33 kb and XII-right ~1060 kb) were not called because they failed to meet the criteria in either wild-type or mutant curves, and are therefore omitted from the plot in Figure 2B. In two cases (at VIII-left and X-left) probable origins failing to meet these criteria were called, based on a falling curve at the terminal data point displaying a drop of greater than 1.5 SD values from the origin value.

### Western blotting

Proteins were extracted as described (Stirling *et al.*, 1994). Ten or fifteen percent polyacrylamide gels were run, and proteins were transferred to a Hybond-P membrane (GE Healthcare Life Sciences, Piscataway, NJ), according to standard methods. For Western blot analysis, membranes were blocked and then incubated for 3 h with primary antibody—anti–acetyl histone H4 K5,8,12,16 (06–598 Lot 29867; Upstate Biotechnology, Lake Placid, NY), anti–acetyl histone H3 K18 (07–354 Lot 27132; Upstate), anti–histone H3 (ab1791 Lot 80051; Abcam, Cambridge, MA), or anti–c-Myc [9E11] (ab56 Lot 191919; Abcam)—then washed, and incubated for 2 h with secondary antibody (either HRP-conjugated anti–mouse [ab6729 Lot 131853; Abcam] or HRP-conjugated anti–rabbit [12–348 Lot 29902; Upstate]) before enhanced chemiluminescence visualization.

### Flow cytometry

Flow cytometry analysis was performed as described by McCune *et al.* (2008).

### ChIP

ChIP was performed as described (Hecht and Grunstein, 1999; Hiraga *et al.*, 2006). Briefly, samples were fixed with formaldehyde for 30 min at room temperature before sonication to an average size of 500 bp. Samples were immunoprecipitated using Dynabeads M-280 sheep anti–rabbit immunoglobulin (Ig)G-112.04 (Invitrogen, Carlsbad, CA) and 10.8 μl of anti–acetyl histone H4 K5,8,12,16 (06–598; Upstate), 1.8 μl of anti–acetyl histone H3 K18 (07–354; Upstate), or 3.6 μl of anti–histone H3 (ab1791; Abcam). Alternatively, 125 μl of Dynabeads Pan Mouse IgG-110.41 (Invitrogen) was used with 10 μl of anti–c-Myc [9E11] (ab56 Lot 191919; Abcam). Precipitated DNA was resuspended in 10 mM Tris, pH 7.5, 1 mM EDTA for use in real-time qPCR.

### Real-Time qPCR

Reactions were run using Finnzymes F-400L qPCR mix on a Roche LightCycler 480 or a DNA Engine Opticon 2 real-time PCR machine, and results were analyzed using Opticon Monitor software (version 3.1; Bio-Rad, Hercules, CA). For each primer pair in each reaction, a threefold dilution series of standard DNA (whole genomic DNA) was run in duplicate. Genomic standard DNA was prepared as for ChIP but omitted the immunoprecipitation step.

For the experiments shown in Figure 5, samples were run as a 1 in 3 dilution series, performed in duplicate. Results were obtained in "DNA units" in comparison to the standard dilution series, where the top dilution "standard" sample was assigned as containing 100 DNA units. Results were then expressed relative to the signal obtained from an internal locus (*PPH3*, which showed consistently similar levels of immunoprecipitation from wild-type and *yku70* mutant chromatin). Error bars in Figure 5 and Supplemental Figure S6 show the range of values between two ChIP experiments. The data shown in Figure 4 and Supplemental Figure S5 plot "raw DNA units" in relation to the standard curves, with the data presented as an average of qPCR duplicates. Primer sequences used in the PCRs are listed in Supplemental Table S3.

## ACKNOWLEDGMENTS

We thank current and past members of the Donaldson and Brewer/Raghuraman laboratories for helpful discussions. Our particular thanks go to Andrew Cosgrove, Conrad Nieduszynski, Walt Fangman, and Ginger Zakian for encouragement and suggestions.

Lorraine Pillus, Maria Vogelauer, Ginger Zakian, John Wyrick, and Vicki Lundblad provided constructs and strains. This work was supported by Cancer Research UK grants C1445/A2571 and C1445/A10817, by Medical Research Council grant G0600774 to A.D.D., and by National Institute of General Medical Sciences grant 18926 to W.L. Fangman, B.J.B., and M.K.R.

## REFERENCES

Alvino GM, Collingwood D, Murphy JM, Delrow J, Brewer BJ, Raghuraman MK (2007). Replication in hydroxyurea: it's a matter of time. Mol Cell Biol 27, 6396–6406.

Aparicio JG, Viggiani CJ, Gibson DG, Aparicio OM (2004). The Rpd3-Sin3 histone deacetylase regulates replication timing and enables intra-S origin control in S. cerevisiae. Mol Cell Biol 24, 4769–4780.

Askree SH, Yehuda T, Smolikov S, Gurevich R, Hawk J, Coker C, Krauskopf A, Kupiec M, McEachern MJ (2004). A genome-wide screen for S. cerevisiae deletion mutants that affect telomere length. Proc Natl Acad Sci USA 101, 8658–8663.

Bianchi A, Shore D (2007). Early replication of short telomeres in budding yeast. Cell 128, 1051–1062.

Bianchi A, Shore D (2008). How telomerase reaches its end: mechanism of telomerase regulation by the telomeric complex. Mol Cell 31, 153–165.

Bochman ML, Sabouri N, Zakian VA (2010). Unwinding the functions of the Pif1 family helicases. DNA Repair 9, 237–249.

Boule JB, Vega LR, Zakian VA (2005). The yeast Pif1p helicase removes telomerase from telomeric DNA. Nature 438, 57–61.

Boulton SJ, Jackson SP (1998). Components of the Ku-dependent nonhomologous end-joining pathway are involved in telomeric length maintenance and telomeric silencing. EMBO J 17, 1819–1828.

Buonomo SB, Wu Y, Ferguson D, de Lange T (2009). Mammalian Rif1 contributes to replication stress survival and homology-directed repair. J Cell Biol 187, 385–398.

Clarke AS, Lowell JE, Jacobson SJ, Pillus L (1999). Esa1p is an essential histone acetyltransferase required for cell cycle progression. Mol Cell Biol 19, 2515–2526.

Cosgrove AJ, Nieduszynski CA, Donaldson AD (2002). Ku complex controls the replication time of DNA in telomere regions. Genes Dev 16, 2485–2490.

Donaldson AD, Fangman WL, Brewer BJ (1998a). Cdc7 is required throughout the yeast S phase to activate replication origins. Genes Dev 12, 491–501.

Donaldson AD, Raghuraman MK, Friedman KL, Cross FR, Brewer BJ, Fangman WL (1998b). CLB5-dependent activation of late replication origins in S. cerevisiae. Mol Cell 2, 173–182.

Evans SK, Lundblad V (1999). Est1 and Cdc13 as comediators of telomerase access. Science 286, 117–120.

Ferguson BM, Brewer BJ, Reynolds AE, Fangman WL (1991). A yeast origin of replication is activated late in S phase. Cell 65, 507–515.

Ferguson BM, Fangman WL (1992). A position effect on the time of replication origin activation in yeast. Cell 68, 333–339.

Fisher TS, Taggart AK, Zakian VA (2004). Cell cycle-dependent regulation of yeast telomerase by Ku. Nat Struct Mol Biol 11, 1198–1205.

Friedman KL, Diller JD, Ferguson BM, Nyland SVM, Brewer BJ, Fangman WL (1996). Multiple determinants controlling activation of yeast replication origins late in S phase. Genes Dev 10, 1595–1607.

Gatbonton T, Imbesi M, Nelson M, Akey JM, Ruderfer DM, Kruglyak L, Simon JA, Bedalov A (2006). Telomere length as a quantitative trait: genome-wide survey and genetic mapping of telomere length-control genes in yeast. PLoS Genet 2, 304–315.

Griffith AJ, Blier PR, Mimori T, Hardin JA (1992). Ku polypeptides synthesized in vitro assemble into complexes which recognize ends of double-stranded DNA. J Biol Chem 267, 331–338.

Hardy CF, Sussel L, Shore D (1992). A RAP1-interacting protein involved in transcriptional silencing and telomere length regulation. Genes Dev 6, 801–814.

Hecht A, Grunstein M (1999). Mapping DNA interaction sites of chromosomal proteins using immunoprecipitation and polymerase chain reaction. Methods Enzymol 304, 399–414.

Hiraga S, Robertson ED, Donaldson AD (2006). The Ctf18 RFC-like complex positions yeast telomeres but does not specify their replication time. EMBO J 25, 1505–1514.

Knott SR, Viggiani CJ, Tavaré S, Aparicio OM (2009). Genome-wide replication profiles indicate an expansive role for Rpd3L in regulating replication initiation timing or efficiency, and reveal genomic loci of Rpd3 function in S. cerevisiae. Genes Dev 23, 1077–1090.

Laroche T, Martin SG, Gotta M, Gorham HC, Pryde FE, Louis EJ, Gasser SM (1998). Mutation of yeast Ku genes disrupts the subnuclear organization of telomeres. Curr Biol 8, 653–656.

Louis EJ (1995). The chromosome ends of Saccharomyces cerevisiae. Yeast 11, 1553–1573.

Maringele L, Lydall D (2002). EXO1-dependent single-stranded DNA at telomeres activates subsets of DNA damage and spindle checkpoint pathways in budding yeast yku70Delta mutants. Genes Dev 16, 1919–1933.

Martin SG, Laroche T, Suka N, Grunstein M, Gasser SM (1999). Relocalization of telomeric Ku and SIR proteins in response to DNA strand breaks in yeast. Cell 97, 621–633.

McCarroll RM, Fangman WL (1988). Time of replication of yeast centromeres and telomeres. Cell 54, 505–513.

McCune HJ, Danielson LS, Alvino GM, Collingwood D, Delrow JJ, Fangman WL, Brewer BJ, Raghuraman MK (2008). The temporal program of chromosome replication: genomewide replication in clb5Δ S. cerevisiae. Genetics 180, 1833–1847.

Nieduszynski CA, Hiraga S, Ak P, Benham C, Donaldson AD (2007). OriDB: a DNA replication origin database. Nucleic Acids Res 35, D40–D46.

Nieduszynski CA, Knox Y, Donaldson AD (2006). Genome-wide identification of replication origins in yeast by comparative genomics. Genes Dev 20, 1874–1879.

Novac O, Matheos D, Araujo FD, Price GB, Zannis-Hadjopoulos M (2001). In vivo association of Ku with mammalian origins of DNA replication. Mol Biol Cell 12, 3386–3401.

Ono M, Tucker PW, Capra JD (1994). Production and characterization of recombinant human Ku antigen. Nucleic Acids Res 22, 3918–3924.

Parnas O, Zipin-Roitman A, Pfander B, Liefshitz B, Mazor Y, Ben-Aroya S, Jentsch S, Kupiec M (2010). Elg1, an alternative subunit of the RFC clamp loader, preferentially interacts with SUMOylated PCNA. EMBO J 29, 2611–2622.

Peterson SE, Stellwagen AE, Diede SJ, Singer MS, Haimberger ZW, Johnson CO, Tzoneva M, Gottschling DE (2001). The function of a stem-loop in telomerase RNA is linked to the DNA repair protein Ku. Nat Genet 27, 64–67.

Pryde F, Jain D, Kerr A, Curley R, Mariotti FR, Vogelauer M (2009). H3 K36 methylation helps determine the timing of Cdc45 association with replication origins. PLoS One 12, e5882.

Raghuraman MK, Brewer BJ, Fangman WL (1997). Cell cycle-dependent establishment of a late replication program. Science 276, 806–809.

Raghuraman MK, Winzeler EA, Collingwood D, Hunt S, Wodicka L, Conway A, Lockhart DJ, Davis RW, Brewer BJ, Fangman WL (2001). Replication dynamics of the yeast genome. Science 294, 115–121.

Reynolds AE, McCarroll RM, Newlon CS, Fangman WL (1989). Time of replication of ARS elements along yeast chromosome III. MolCell Biol 9, 4488–4494.

Robyr D, Suka Y, Xenarios I, Kurdistani SK, Wang A, Suka N, Grunstein M (2002). Microarray deacetylation maps determine genome-wide functions for yeast histone deacetylases. Cell 109, 437–446.

Shakibai N, Kumar V, Eisenberg S (1996). The Ku-like protein from Saccharomyces cerevisiae is required in vitro for the assembly of a stable multiprotein complex at a eukaryotic origin of replication. Proc Natl Acad Sci USA 93, 11569–11574.

Stellwagen AE, Haimberger ZW, Veatch JR, Gottschling DE (2003). Ku interacts with telomerase RNA to promote telomere addition at native and broken chromosome ends. Genes Dev 17, 2384–2395.

Stevenson JB, Gottschling DE (1999). Telomeric chromatin modulates replication timing near chromosome ends. Genes Dev 13, 146–151.

Stirling DA, Welch KA, Stark MJR (1994). Interaction with calmodulin is required for the function of Spc110p, an essential component of the yeast spindle pole body. EMBO J 13, 4329–4342.

Vogelauer M, Rubbi L, Lucas I, Brewer BJ, Grunstein M (2002). Histone acetylation regulates the time of replication origin firing. Mol Cell 10, 1223–1233.

Wotton D, Shore D (1997). A novel Rap1p-interacting factor, Rif2p, cooperates with Rif1p to regulate telomere length in S. cerevisiae. Genes Dev 11, 748–760.

Yabuki N, Terashima H, Kitada K (2002). Mapping of early firing origins on a replication profile of budding yeast. Genes Cells 7, 781–789.

Zhou J, Monson EK, Teng SC, Schulz VP, Zakian VA (2000). Pif1p helicase, a catalytic inhibitor of telomerase in yeast. Science 289, 771–774.